Bentamy A, Queffeulou P, Quilfen Y and Katsaros KB (1999) Ocean surface wind fields estimated from satellite active and passive microwave instruments. *IEEE Transactions Geosci Remote Sens*. 37: 2469–2486.

de Leeuw G (1990) Profiling of aerosol concentrations, particle size distributions, and relative humidity in the atmospheric surface layer over the North Sea. *Tellus* 42B: 342–354.

Dobson F, Hasse L and Davies R (eds) (1980) *Instruments and Methods in Air–Sea Interaction*, pp. 293–317. New York: Plenum.

Geernaert GL and Plant WJ (eds) (1990) *Surface Waves and Fluxes*, vol. 2, pp. 339–368. Dordrecht: Kluwer Academic Publishers.

Graf J, Sasaki C, *et al*. (1998) NASA Scatterometer Experiment. *Asta Astronautica* 43: 397–407.

Gruber A, Su X, Kanamitsu M and Schemm J (2000) The comparison of two merged rain gauge-satellite precipitation datasets. *Bulletin of the American Meteorological Society* 81: 2631–2644.

Katsaros KB (1980) Radiative sensing of sea surface temperatures. In: Dobson F, Hasse L and Davies R (eds) *Instruments and Methods in Air–sea* Interaction, pp. 293–317. New York: Plenum Publishing Corp.

Katsaros KB, DeCosmo J, Lind RJ *et al*. (1994) Measurements of humidity and temperature in the marine environment. *Journal of Atmospheric and Oceanic Technology* 11: 964–981.

Kummerow C, Barnes W, Kozu T, Shiue J and Simpson J (1998) The tropical rainfall measuring mission (TRMM) sensor package. *Journal of Atmospheric and Oceanic Technology* 15: 809–817.

Liu WT (1990) Remote sensing of surface turbulence flux. In: Geenaert GL and Plant WJ (eds) *Surface Waves and Fluxes*, vol. 2, pp. 293–309. Dordrecht: Kluwer Academic Publishers.

Parker SP (ed.) (1977) *Encyclopedia of Ocean and Atmospheric Science*. New York: McGraw-Hill.

Pinker RT and Laszlo I (1992) Modeling surface solar irradiance for satellite applications on a global scale. *Journal of Applied Meteorology* 31: 194–211.

Reynolds RR and Smith TM (1994) Improved global sea surface temperature analyses using optimum interpolation. *Journal of Climate* 7: 929–948.

List RJ (1958) *Smithsonian Meteorological Table*s, 6th edn. City of Washington: Smithsonian Institution Press.

van der Meulen JP (1988) On the need of appropriate filter techniques to be considered using electrical humidity sensors. In: *Proceedings of the WMO Technical Conference on Instruments and Methods of Observation (TECO-1988)*, pp. 55–60. Leipzig, Germany: WMO.

Wentz FJ and Smith DK (1999) A model function for the ocean-normalized radar cross-section at 14 GHz derived from NSCAT observations. *Journal of Geophysical Research* 104: 11 499–11 514.

SENSORS FOR MICROMETEOROLOGICAL FLUX MEASUREMENTS

J. B. Edson, Woods Hole Oceanographic Institution, Woods Hole, MA, USA

doi:10.1006/rwos.2001.0330

Introduction

The exchange of momentum, heat, and mass between the atmosphere and ocean is the fundamental physical process that defines air–sea interactions. This exchange drives ocean and atmospheric circulations, and generates surface waves and currents. Marine micrometeorologists are primarily concerned with the vertical exchange of these quantities, particularly the vertical transfer of momentum, heat, moisture, and trace gases associated with the momentum, sensible heat, latent heat, and gas fluxes, respectively. The term flux is defined as the amount of heat (i.e., thermal energy) or momentum transferred per unit area per unit time.

Air–sea interaction studies often investigate the dependence of the interfacial fluxes on the mean meteorological (e.g., wind speed, degree of stratification or convection) and surface conditions (e.g., surface currents, wave roughness, wave breaking, and sea surface temperature). Therefore, one of the goals of these investigations is to parametrize the fluxes in terms of these variables so that they can be incorporated in numerical models. Additionally, these parametrizations allow the fluxes to be indirectly estimated from observations that are easier to collect and/or offer wider spatial coverage. Examples include the use of mean meteorological measurements from buoys or surface roughness measurements from satellite-based scatterometers to estimate the fluxes.

Direct measurements of the momentum, heat, and moisture fluxes across the air–sea interface are crucial to improving our understanding of the coupled atmosphere–ocean system. However, the operating requirements of the sensors, combined with the often harsh conditions experienced over the ocean, make this a challenging task. This article begins with a description of desired measurements and the

operating requirements of the sensors. These requirements involve adequate response time, reliability, and survivability. This is followed by a description of the sensors used to meet these requirements, which includes examples of some of the obstacles that marine researchers have had to overcome. These obstacles include impediments caused by environmental conditions and engineering challenges that are unique to the marine environment. The discussion is limited to the measurement of velocity, temperature, and humidity. The article concludes with a description of the state-of-the-art sensors currently used to measure the desired fluxes.

Flux Measurements

The exchange of momentum and energy a few meters above the ocean surface is dominated by turbulent processes. The turbulence is caused by the drag (i.e., friction) of the ocean on the overlying air, which slows down the wind as it nears the surface and generates wind shear. Over time, this causes faster-moving air aloft to be mixed down and slower-moving air to be mixed up; the net result is a downward flux of momentum. This type of turbulence is felt as intermittent gusts of wind that buffet an observer looking out over the ocean surface on a windy day.

Micrometeorologists typically think of these gusts as turbulent eddies in the airstream that are being advected past the observer by the mean wind. Using this concept, the turbulent fluctuations associated with these eddies can be defined as any departure from the mean wind speed over some averaging period (eqn [1]).

$$u(t) = U(t) - \bar{U} \qquad [1]$$

In eqn [1], $u(t)$ is the fluctuating (turbulent) component, $U(t)$ is the observed wind, and the overbar denotes the mean value over some averaging period. The fact that an observer can be buffeted by the wind indicates that these eddies have some momentum. Since the eddies can be thought to have a finite size, it is convenient to consider their momentum per unit volume, given by $\rho_a U(t)$, where ρ_a is the density of air. In order for there to be an exchange of momentum between the atmosphere and ocean, this horizontal momentum must be transferred downward by some vertical velocity. The mean vertical velocity associated with the turbulent flux is normally assumed to be zero. Therefore, the turbulent transfer of this momentum is almost exclusively via the turbulent vertical velocity, $w(t)$, which we associate with overturning air.

The correlation or covariance between the fluctuating vertical and horizontal wind components is the most direct estimate of the momentum flux. This approach is known as the eddy correlation or direct covariance method. Computation of the covariance involves multiplying the instantaneous vertical velocity fluctuations with one of the horizontal components. The average of this product is then computed over the averaging period.

Because of its dependence on the wind shear, the flux of momentum at the surface is also known as the shear stress defined by eqn [2], where $\hat{\mathbf{i}}$ and $\hat{\mathbf{j}}$ are unit vectors, and v is the fluctuating horizontal component that is orthogonal to u.

$$\tau_0 = \hat{\mathbf{i}}\overline{uw} - \hat{\mathbf{j}}\overline{vw} \qquad [2]$$

Typically, the coordinate system is rotated into the mean wind such that u, v, and w denote the longitudinal, lateral, and vertical velocity fluctuations, respectively. Representative time series of longitudinal and vertical velocity measurements taken in the marine boundary layer are shown in **Figure 1**. The velocities in this figure exhibit the general trend that downward-moving air (i.e., $w < 0$) is transporting eddies with higher momentum per unit mass (i.e., $\rho_a u > 0$) and vice versa. The overall correlation is therefore negative, which is indicative of a downward flux of momentum.

Close to the surface, the wave-induced momentum flux also becomes important. At the interface, the turbulent flux actually becomes negligible and the momentum is transferred via wave drag and viscous shear stress caused by molecular viscosity.

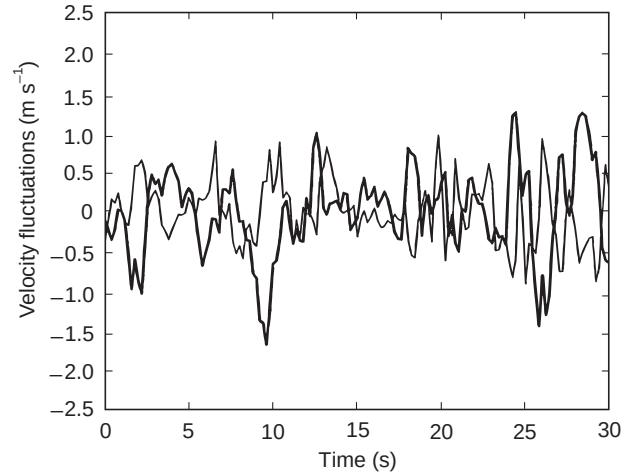

Figure 1 Time-series of the longitudinal (thick line) and vertical velocity (thin line) fluctuations measured from a stable platform. The mean wind speed during the sampling period was 10.8 m s^{-1}.

The ocean is surprisingly smooth compared to most land surfaces. This is because the dominant roughness elements that cause the drag on the atmosphere are the wind waves shorter than 1 m in length. Although the longer waves and swell give the appearance of a very rough surface, the airflow tends to follow these waves and principally act to modulate the momentum flux supported by the small-scale roughness. Therefore, the wave drag is mainly a result of these small-scale roughness elements.

Turbulence can also be generated by heating and moistening the air in contact with the surface. This increases the buoyancy of the near-surface air, and causes it to rise, mix upward, and be replaced by less-buoyant air from above. The motion generated by this convective process is driven by the surface buoyancy flux (eqn [3]).

$$B_0 = \rho_a c_p \overline{w\theta_v} \qquad [3]$$

In eqn [3] c_p is the specific heat of air at constant pressure and θ_v is the fluctuating component of the virtual potential temperature defined in eqn [4], where $\bar{\Theta}$ and θ are the mean and fluctuating components of the potential temperature, respectively, and q is the specific humidity (i.e., the mass of water vapor per unit mass of moist air).

$$\theta_v = \theta + 0.61\bar{\Theta}q \qquad [4]$$

These quantities also define the sensible heat (eqn [5]) and latent heat (eqn [6]) fluxes.

$$H_0 = \rho_a c_p \overline{w\theta} \qquad [5]$$

$$E_0 = L_e \overline{w\rho_a q} \qquad [6]$$

where L_e is the latent heat of evaporation. The parcels of air that are heated and moistened via the buoyancy flux can grow into eddies that span the entire atmospheric boundary layer. Therefore, even in light wind conditions with little mean wind shear, these turbulent eddies can effectively mix the marine boundary layer.

Conversely, when the air is warmer than the ocean, the flow of heat from the air to water (i.e., a downward buoyancy flux) results in a stably stratified boundary layer. The downward buoyancy flux is normally driven by a negative sensible heat flux. However, there have been observations of a downward latent heat (i.e., moisture) flux associated with the formation of fog and possibly condensation at the ocean surface. Vertical velocity fluctuations have to work to overcome the stratification since upward-moving eddies are trying to bring up denser air and vice versa. Therefore, stratified boundary layers tend to dampen the turbulent fluctuations and reduce the flux compared to their unstable counterpart under similar mean wind conditions. Over the ocean, the most highly stratified stable boundary layers are usually a result of warm air advection over cooler water. Slightly stable boundary conditions can also be driven by the diurnal cycle if there is sufficient radiative cooling of the sea surface at night.

Sensors

Measurement of the momentum, sensible heat, and latent heat fluxes requires a suite of sensors capable of measuring the velocity, temperature, and moisture fluctuations. Successful measurement of these fluxes requires instrumentation that is rugged enough to withstand the harsh marine environment and fast enough to measure the entire range of eddies that transport these quantities. Near the ocean surface, the size of the smallest eddies that can transport these quantities is roughly half the distance to the surface; i.e., the closer the sensors are deployed to the surface, the faster the required response. In addition, micrometeorologists generally rely on the wind to advect the eddies past their sensors. Therefore, the velocity of the wind relative to a fixed or moving sensor also determines the required response; i.e., the faster the relative wind, the faster the required response. For example, planes require faster response sensors than ships but require less averaging time to compute the fluxes because they sample the eddies more quickly.

The combination of these two requirements results in an upper bound for the required frequency response (eqn [7]).

$$\frac{fz}{U_r} \approx 2 \qquad [7]$$

Here f is the required frequency response, z is the height above the surface, and U_r is the relative velocity. As a result, sensors used on ships, buoys, and fixed platforms require a frequency response of approximately 10–20 Hz, otherwise some empirical correction must be applied. Sensors mounted on aircraft require roughly an order of magnitude faster response depending on the sampling speed of the aircraft.

The factors that degrade sensor performance in the marine atmosphere include contamination, corrosion, and destruction of sensors due to sea spray

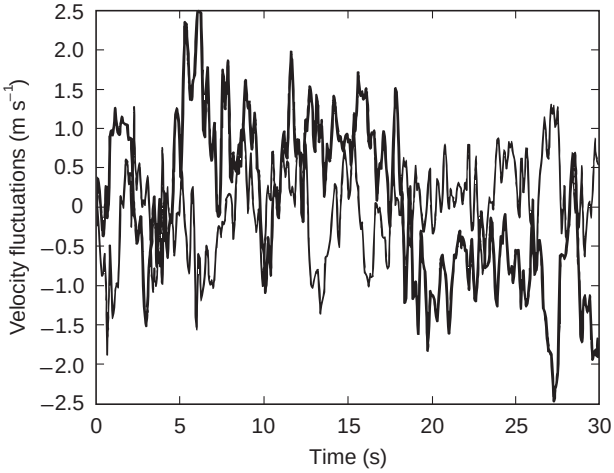

Figure 2 Time-series of the longitudinal (thick line) and vertical velocity (thin line) fluctuations measured from a 3 m discus buoy. The mean wind speed during the sampling period was 10.9 m s^{-1}. The measured fluctuations are a combination of turbulence and wave-induced motion of the buoy.

and salt water; and fatigue and failure caused by long-term operation that is accelerated on moving platforms. Additionally, if the platform is moving, the motion of the platform will be sensed by the instrument as an additional velocity and will contaminate the desired signal (**Figure 2**). Therefore, the platform motion must be removed to accurately measure the flux. This requires measurements of the linear and angular velocity of the platform. The alternative is to deploy the sensors on fixed platforms or to reduce the required motion correction by mounting the sensors on spar buoys, SWATH vessels, or other platforms that are engineered to reduced the wave-induced motion.

Shear Stress

The measurement of momentum flux or shear stress has a long history. The earliest efforts attempted to adapt many of the techniques commonly used in the laboratory to the marine boundary layer. A good example of this is the use of hot-wire anemometers that are well-suited to wind tunnel studies of turbulent flow. Hot-wire anemometry relies on very fine platinum wires that provide excellent frequency response and satisfy eqn [7] even close to the surface. The technique relies on the assumption that the cooling of heated wires is proportional to the flow past the wire. Hot-wire anemometers are most commonly used in constant-temperature mode. In this mode of operation, the current heating the wire is varied to maintain a constant temperature using a servo loop. The amount of current or power required to maintain the temperature is a measure of the cooling of the wires by the wind.

Unfortunately, there are a number of problems associated with the use of these sensors in the marine environment. The delicate nature of the wires (they are typically 10 μm in diameter) makes them very susceptible to breakage. Hot-film anemometers provide a more rugged instrument with somewhat slower, but still excellent, frequency response. Rather than strands of wires, a hot-film anemometer uses a thin film of nickel or platinum spread over a small cylindrical quartz or glass core. Even when these sensors are closely monitored for breakage, aging and corrosion of the wires and films due to sea spray and other contaminants cause the calibration to change over time. Dynamic calibration in the field has been used but this requires additional sensors. Therefore, substantially more rugged anemometers with absolute or more stable calibrations have generally replaced these sensors in field studies.

Another laboratory instrument that meets these requirements is the pitot tube; this uses two concentric tubes to measure the difference between the static pressure of the inner tube, which acts as a stagnation point, and the static pressure of the air flowing past the sensor. The free stream air also has a dynamic pressure component. Therefore, the difference between the two pressure measurements can be used to compute the dynamic pressure of the air flow moving past the sensor using Bernoulli's equation (eqn [8]).

$$\Delta p = \frac{1}{2}\rho_a \alpha U^2 \qquad [8]$$

Here α is a calibration coefficient that corrects for departures from Bernoulli's equations due to sensor geometry. A calibrated pitot tube can then be used to measure the velocity.

The traditional design is most commonly used to measure the streamwise velocity. However, three-axis pressure sphere (or cone) anemometers have been used to measure fluxes in the field. These devices use a number of pressure ports that are referenced against the stagnation pressure to measure all three components of the velocity. This type of anemometer has to be roughly aligned with the relative wind and its ports must remain clear of debris (e.g., sea spray and other particulates) to operate properly. Consequently, it has been most commonly used on research aircraft where the relative wind is large and particulate concentrations are generally lower outside of clouds and fog.

The thrust anemometer has also been used to directly measure the momentum flux in the marine

Figure 3 The instrument at the far right is a K-Gill anemometer shown during a deployment on a research vessel. The instrument on the left is a sonic anemometer that is shown in more detail in **Figure 4**. Photograph provided by Olc Persson (CIRES/NOAA/ETL).

Figure 4 A commercially available pulse-type sonic anemometer. The three sets of paired transducers are cabable of measuring the three components of the velocity vector. This type of device produced the time-series in **Figure 1** and **Figure 2**. The sonic anemometer measures 0.75 m from top to bottom.

atmosphere. This device measures the frictional drag of the air on a sphere or other objects. The most successful design uses springs to attach a sphere and its supporting structure to a rigid mount. The springs allow the sphere to be deflected in both the horizontal and vertical directions. The deflection due to wind drag on the sphere is sensed by proximity sensors that measure the displacement relative to the rigid mount. Carefully calibrated thrust anemometers have been used to measure turbulence from fixed platforms for extended periods. They are fairly rugged and low-power, and have adequate response for estimation of the flux. The main disadvantages of these devices are the need to accurately calibrate the direction response of each sensor and sensor drift due to aging of the springs.

A very robust sensor for flux measurements, particularly for use on fixed platforms, relies on a modification of the standard propellor vane anemometer used to measure the mean wind. The modification involves the use of two propellers on supporting arms set at 90° to each other. The entire assembly is attached to a vane that keeps the propeller pointed into the wind. The device is known as a K-Gill anemometer from the appearance of the twin propeller-vane configuration (**Figure 3**). The twin propellers are capable of measuring the instantaneous vertical and streamwise velocity, and the vane reading allows the streamwise velocity to be broken down into its u and v components. This device is also very robust and low power. However, it has a complicated inertial response on moving platforms and is therefore most appropriate for use on fixed platforms. Additionally, the separation between the propellers (typically 0.6 m) acts as a spatial filter (i.e., it cannot detect eddies smaller than the separation), so it cannot be used too close to the surface and still satisfy eqn [7]. This is generally not a problem at the measurement heights used in most field deployments.

Over the past decade, sonic anemometers have become the instrument of choice for most investigations of air–sea interaction. These anemometers use acoustic signals that are emitted in either a continuous or pulsed mode. At present, the pulse type sonic anemometers are most commonly used in marine research. Most commercially available devices use paired transducers that emit and detect acoustic pulses (**Figure 4**). One transducer emits the pulse and the other detects it to measure the time of flight between them. The functions are then reversed to measure the time of flight in the other direction. The

basic concept is that in the absence of any wind the time of flight in either direction is the same. However, the times of flight differ if there is a component of the wind velocity along the path between the transducers. The velocity is directly computed from the two time of flight measurements, t_1 and t_2, using eqn [9], where L is the distance between the transducers.

$$U = \frac{L}{2}\left(\frac{1}{t_1} - \frac{1}{t_2}\right) \qquad [9]$$

Three pairs of transducers are typically used to measure all three components of the velocity vector. These devices have no moving parts and are therefore far less susceptible to mechanical failure. They can experience difficulties when rain or ice covers the transducer faces or when there is a sufficient volume of precipitation in the sampling volume. However, the current generation of sonic anemometers have proven themselves to be remarkably reliable in long-term deployments over the ocean; so much so that two-axis versions of sonic anemometers are also beginning to replace cup and propellor/vane anemometers for mean wind measurements over the ocean.

Motion Correction

The measurement of the fluctuating velocity components necessary to compute the fluxes is complicated by the platform motion on any aircraft, sea-going research vessel, or surface mooring. This motion contamination must be removed before the fluxes can be estimated. The contamination of the signal arises from three sources: instantaneous tilt of the anemometer due to the pitch, roll, and yaw (i.e., heading) variations; angular velocities at the anemometer due to rotation of the platform about its local coordinate system axes; and translational velocities of the platform with respect to a fixed frame of reference. Therefore, motion sensors capable of measuring these quantities are required to correct the measured velocities. Once measured, these variables are used to compute the true wind vector from eqn [10].

$$\mathbf{U} = \boldsymbol{T}(\mathbf{U}_m + \boldsymbol{\Omega}_m \times \mathbf{R}) + \mathbf{U}_p \qquad [10]$$

Here $\mathbf{U}$ is the desired wind velocity vector in the desired reference coordinate system (e.g., relative to water or relative to earth); $\mathbf{U}_m$ and $\boldsymbol{\Omega}_m$ are the measured wind and platform angular velocity vectors respectively, in the platform frame of reference; $\boldsymbol{T}$ is the coordinate transformation matrix from the platform coordinate system to the reference coordinates; $\mathbf{R}$ is the position vector of the wind sensor with respect to the motion sensors; and $\mathbf{U}_p$ is the translational velocity vector of the platform measured at the location of the motion sensors.

A variety of approaches have been used to correct wind sensors for platform motion. True inertial navigation systems are standard for research aircraft. These systems are expensive, so simpler techniques have been sought for ships and buoys, where the mean vertical velocity of the platform is unambiguously zero. These techniques generally use the motion measurements from either strapped-down or gyro-stabilized systems.

The strapped-down systems typically rely on a system of three orthogonal angular rate sensors and accelerometers, which are combined with a compass to get absolute direction. The high-frequency component of the pitch, roll, and yaw angles required for the transformation matrix are computed by integrating and highpass filtering the angular rates. The low-frequency component is obtained from the lowpass accelerometer signals or, more recently, the angles computed from differential GPS. The transformed accelerometers are integrated and highpass filtered before they are added to lowpass filtered GPS or current meter velocities for computation of $\mathbf{U}_p$ relative to earth or the sea surface, respectively. The gyro-stabilized system directly computes the orientation angles of the platform. The angular rates are then computed from the time-derivative of the orientation angles.

Heat Fluxes

The measurement of temperature fluctuations over the ocean surface has a similar history to that of the velocity measurements. Laboratory sensors such as thermocouples, thermistors, and resistance wires are used to measure temperature fluctuations in the marine environment.

Thermocouples rely on the Seebeck effect that arises when two dissimilar materials are joined to form two junctions: a measuring junction and a reference junction. If the temperature of the two junctions is different, then a voltage potential difference exists that is proportional to the temperature difference. Therefore, if the temperature of the reference junction is known, then the absolute temperature at the measuring junction can be determined. Certain combinations of materials exhibit a larger effect (e.g., copper and constantan) and are thus commonly used in thermocouple design. However, in all cases the voltage generated by the thermoelectric effect is small and amplifiers are often used along with the probes.

Thermistors and resistance wires are devices whose resistance changes with temperature. Thermistors are semiconductors that generally exhibit a large negative change of resistance with temperature (i.e., they have a large negative temperature coefficient of resistivity). They come in a variety of different forms including beads, rods, or disks. Microbead thermistors are most commonly used in turbulence studies; in these the semiconductor is situated in a very fine bead of glass. Resistance wires are typically made of platinum, which has a very stable and well-known temperature–resistance relationship. The trade-off is that they are less sensitive to temperature change than thermistors. The probe supports for these wires are often similar in design to hot-wire anemometers, and they are often referred to as cold-wires.

All of these sensors can be deployed on very fine mounts (**Figure 5**), which greatly reduces the adverse effects of solar heating but also exposes them to harsh environments and frequent breaking. Additionally, the exposure invariably causes them to become covered with salt from sea spray. The coating of salt causes spurious temperature fluctuations due to condensation and evaporation of water vapor on these hygroscopic particles. These considerations generally require more substantial mounts and some sort of shielding from the radiation and spray.

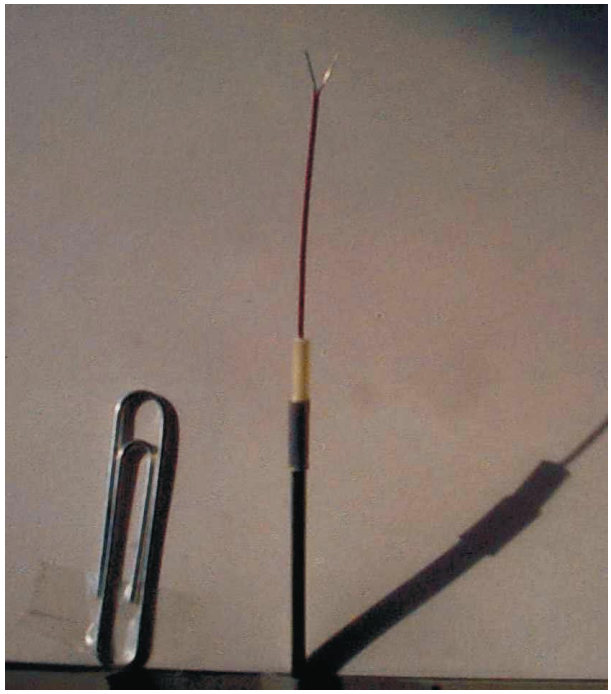

Figure 5 A thermocouple showing the very fine mounts used for turbulence applications. The actual thermocouple is situated on fine wires between the probe supports and is too small to be seen in this photograph.

While this is acceptable for mean temperature measurements, the reduction in frequency response caused by the shields often precludes their use for turbulence measurements.

To combat these problems, marine micrometeorologists have increasingly turned to sonic thermometry. The time of flight measurements from sonic anemometers can be used to measure the speed of sound c along the acoustic path (eqn [11]).

$$c = \frac{L}{2}\left(\frac{1}{t_1} + \frac{1}{t_2}\right) \qquad [11]$$

The speed of sound is a function of temperature and humidity and can be used to compute the sonic temperature T_s defined by eqn [12], where U_N is velocity component normal to the transducer path.

$$T_s = T(1 + 0.51q) = \frac{c^2 + U_N^2}{403} \qquad [12]$$

The normal wind term corrects for lengthening of the acoustic path by this component of the wind. This form of velocity crosstalk has a negligible effect on the actual velocity measurements, but has a measurable effect on the sonic temperature.

Sonic thermometers share many of the positive attributes of sonic anemometers. Additionally, they suffer the least from sea salt contamination compared to other fast-response temperature sensors. The disadvantage of these devices is that velocity crosstalk must be corrected for and they do not provide the true temperature signal as shown by eqn [12]. Fortunately, this can be advantageous in many investigations because the sonic temperature closely approximates the virtual temperature in moist air $T_v = T(1 + 0.61q)$. For example, in many investigations over the ocean an estimate of the buoyancy flux is sufficient to account for stability effects. In these investigations the difference between the sonic and virtual temperature is often neglected (or a small correction is applied), and the sonic anemometer/thermometer is all that is required. However, due to the importance of the latent heat flux in the total heat budget over the ocean, accurate measurement of the moisture flux is often a crucial component of air–sea interaction investigations.

The accurate measurement of moisture fluctuations required to compute the latent heat flux is arguably the main instrumental challenge facing marine micrometeorologists. Sensors with adequate frequency response generally rely on the ability of water vapor in air to strongly absorb certain wavelengths of radiation. Therefore, these devices

require a narrowband source for the radiation and a detector to measure the reduced transmission of that radiation over a known distance.

Early hygrometers of this type generated and detected ultraviolet radiation. The Lyman α hygrometer uses a source tube that generates radiation at the Lyman α line of atomic hydrogen which is strongly absorbed by water vapor. This device has excellent response characteristics when operating properly. Unfortunately, it has proven to be difficult to operate in the field due to sensor drift and contamination of the special optical windows used with the source and detector tubes. A similar hygrometer that uses krypton as its source has also been used in the field. Although the light emitted by the krypton source is not as sensitive to water vapor, the device still has more than adequate response characteristics and generally requires less maintenance than the Lyman α. However, it still requires frequent calibration and cleaning of the optics. Therefore, neither device is particularly well suited for long-term operation without frequent attention.

Commercially available infrared hygrometers are being used more and more in marine micrometeorological investigations (**Figure 6**). Beer's law (eqn [13]) provides the theoretical basis for the transmission of radiation over a known distance.

$$T = \mathrm{e}^{-(\gamma+\delta)D} \qquad [13]$$

Here T is the transmittance of the medium, D is the fixed distance, and γ and δ are the extinction coefficients for scattering and absorption, respectively. This law applies to all of the radiation source described above; however, the use of filters with infrared devices allows eqn [13] to be used more directly. For example, the scattering coefficient has a weak wavelength dependence in the spectral region where infrared absorption is strongly wavelength dependent. Filters can be designed to separate the infrared radiation into wavelengths that exhibit strong and weak absorption. The ratio of transmittance of these two wavelengths is therefore a function of the absorption (eqn [14]), where the subscripts s and w identify the variables associated with the strongly and weakly absorbed wavelengths.

$$\frac{T_\mathrm{s}}{T_\mathrm{w}} \approx \mathrm{e}^{-\delta_\mathrm{s} D} \qquad [14]$$

Calibration of this signal then provides a reliable measure of water vapor due to the stability of current generation of infrared sources.

Infrared hygrometers are still optical devices and can become contaminated by sea spray and other airborne contaminants. To some extent the use of the transmission ratio negates this problem if the contamination affects the two wavelengths equally. Obviously, this is not the case when the optics become wet from rain, fog, or spray. Fortunately, the devices recover well once they have dried off and are easily cleaned by the rain itself or by manual flushing with water. Condensation on the optics can also be reduced by heating their surfaces. These devices require longer path lengths (0.2–0.6 m) than Lyman α or krypton hygrometers to obtain measurable absorption (**Figure 6**). This is not a problem as long as they are deployed at heights $\gg D$.

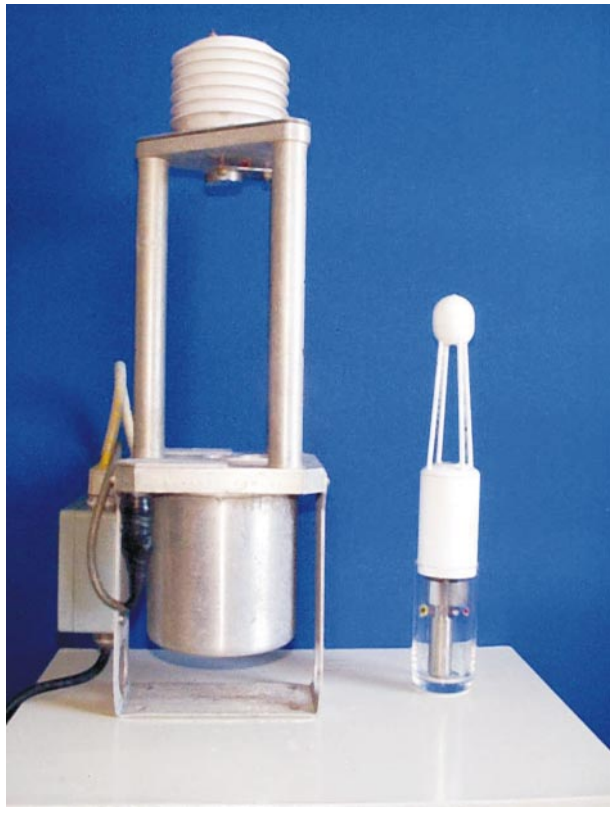

Figure 6 Two examples of commercially available infrared hygrometers. The larger hygrometer is roughly the height of the sonic anemometer shown in **Figure 4**.

Conclusions

The state of the art in sensor technology for use in the marine surface layer includes the sonic anemometer/thermometer and the latest generation of infrared hygrometers (**Figure 7**). However, the frequency response of these devices, mainly due to spatial averaging, precludes their use from aircraft. Instead, aircraft typically rely on gust probes for

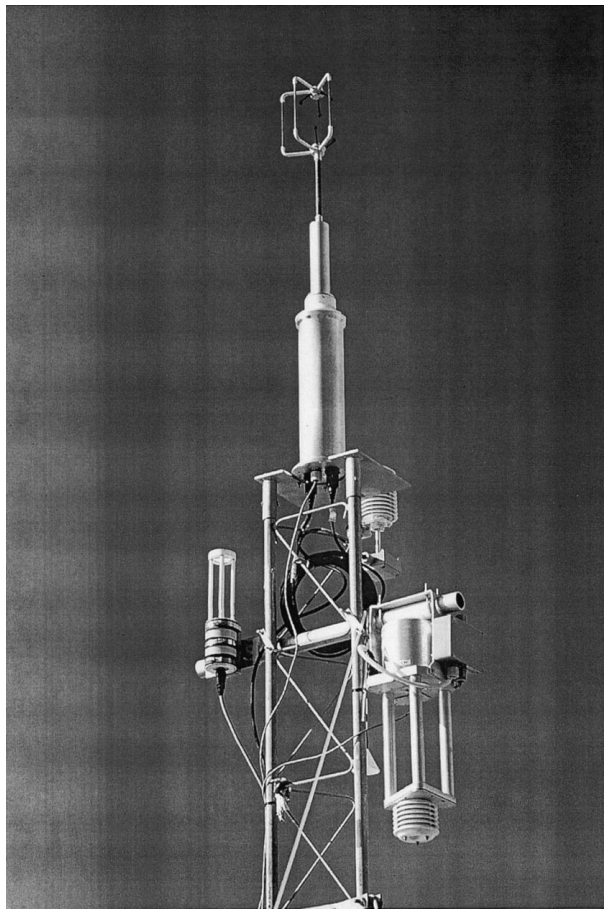

Figure 7 A sensor package used to measure the momentum, sensible heat, and latent heat fluxes from a moving platform. The cylinder beneath the sonic anemometer/thermometer holds 3-axis angular rate sensors and linear accelerometers, as well as a magnetic compass. Two infrared hygrometers are deployed beneath the sonic anemometer. The radiation shield protects sensors that measure the mean temperature and humidity. Photograph provided by Wade McGillis (WHOI).

measurement of the required velocity fluctuations, thermistors for temperature fluctuations, and Lyman α hygrometers for moisture fluctuations. Hot-wire and hot-film anemometers along with the finer temperature and humidity devices are also required to measure directly the viscous dissipation of the turbulent eddies that occurs at very small spatial scales.

Instruments for measuring turbulence are generally not considered low-power when compared to the mean sensors normally deployed on surface moorings, so past deployments of these sensors were mainly limited to fixed platforms or research vessels with ample power. Recently, however, sensor packages mounted on spar and discus buoys have successfully measured motion-corrected momentum and buoyancy fluxes on month- to year-long deployments with careful power management. The use of these sensor packages is expected to continue owing to the desirability of these measurements and technological advances leading to improved power sources and reduced power consumption by the sensors.

See also

Air–Sea Gas Exchange. Breaking Waves and Near-surface Turbulence. Heat and Momentum Fluxes at the Sea Surface. Moorings. Rigs and Offshore Structures. Satellite Remote Sensing Microwave Scatterometers. Sensors for Mean Meteorology. Ships. Surface, Gravity and Capillary Waves. Turbulence Sensors. Upper Ocean Heat and Freshwater Budgets. Upper Ocean Mixing Processes. Wave Generation by Wind. Wind and Buoyancy-forced Upper Ocean. Wind Driven Circulation.

Further Reading

Ataktürk SS and Katsaros KB (1989) The K-Gill, a twin propeller-vane anemometer for measurements of atmospheric turbulence. *Journal of Atmospheric and Oceanic Technology* 6: 509–515.

Buck AL (1976) The variable path Lyman-alpha hygrometer and its operating characteristics. *Bulletin of the American Meteorological Society* 57: 1113–1118.

Crawford TL and Dobosy RJ (1992) A sensitive fast-response probe to measure turbulence and heat flux from any airplane. *Boundary-Layer Meteorology* 59: 257–278.

Dobson FW, Hasse L and Davis RE (1980) *Air–Sea Interaction; Instruments and Methods*. New York: Plenum Press.

Edson JB, Hinton AA, Prada KE, Hare JE and Fairall CW (1998) Direct covariance flux estimates from mobile platforms at sea. *Journal of Atmospheric and Oceanic Technology* 15: 547–562.

Fritschen LJ and Gay LW (1979) *Environmental Instrumentation*. New York: Springer-Verlag.

Kaimal JC and Gaynor JE (1991) Another look at sonic thermometry. *Boundary-Layer Meteorology* 56: 401–410.

Larsen SE, Højstrup J and Fairall CW (1986) Mixed and dynamic response of hot wires and measurements of turbulence statistics. *Journal of Atmospheric and Oceanic Technology* 3: 236–247.

Schmitt KF, Friehe CA and Gibson CH (1978) Humidity sensitivity of atmospheric temperature sensors by salt contamination. *Journal of Physical Oceanography* 8: 141–161.

Schotanus P, Nieuwstadt FTM, de Bruin HAR (1983) Temperature measurement with a sonic anemometer and its application to heat and moisture fluxes. *Boundary-Layer Meteorology* 26: 81–93.